CHAPTER IV

Surface Capture of N-Terminally Functionalized Proteins out of Lysate

ABSTRACT

In this chapter, we focus on the covalent conjugation of N-terminally labeled proteins to functionalized slides for the creation of protein microarrays. Specifically, 12-ADA-labeled yARF-GFP, CaN, and hCaNB-CaM, prepared via bacterial co-expression with NMT, were selectively coupled to cyclooctyne-spotted glass slides. Moreover, rapid surface capture was achieved directly out of lysate, without prior purification of the recombinantly expressed proteins. Our ability to prepare protein microarrays directly from cellular extracts exploits the orthogonality of NMT toward bacterial systems and the exquisite selectivity of NMT toward both natural and engineered substrate proteins. We also describe experiments completed with an azide dye and acetylene- or cyclooctyne-derivatized agarose beads, which informed our subsequent work with microarrays; these studies provided a comparison of the relative efficiency of reacting azides with terminal alkynes versus cyclic strained alkynes, and they shed light on how reaction efficiency is affected by the presence of lysate proteins.

The microarray studies described in this chapter were performed at Maven Biotechnologies in collaboration with Dr. Tamara Kinzer-Ursem. Maven has developed an instrument for protein measurements based on a technology called LFIRE, or Label-Free Internal Reflection Ellipsometry. Successful coupling of our 12-ADA-labeled proteins to slides was confirmed using the LFIRE instrument, which enables sensitive and high-throughput detection of changes in height on the surface of a slide. Our results in this area provide a strong foundation for future work evaluating the biochemical activity of CaM, CaN, and other labeled proteins in a microarray format.

INTRODUCTION

Immobilization of Proteins on Surfaces

Protein chips and microarrays have been utilized in a variety of contexts. They may serve as components in medical diagnostic systems,[1–3] and they may be useful research tools for *in vitro* studies of the interactions of proteins with small molecules and other proteins.[4–7] Elucidating such interactions is a key step toward discovering new small-molecule drugs that bind specific protein targets and dissecting intricate protein–protein networks that govern complex biological processes, such as memory formation, and disease states, such as oncogenesis.

As such, the development of techniques to couple proteins to surfaces has been an area of active research for the past twenty years, continuing to the present day.[8–10] In 2000, the Schreiber Lab published a landmark paper describing the immobilization of proteins on aldehyde slides via lysine (Lys) side-chain amines.[11] While this work represented a major advance at the time for high-throughput studies of protein-protein interactions, it also utilized a chemical reaction that is neither site-specific nor selective for a single protein: Lys residues are prevalent across the proteome and are often found at multiple sites within a single protein. The use of the Lys-aldehyde reaction and other non-specific protein chemistries yields microarrays that display the protein of interest in various orientations, depending on the site of surface attachment on the protein; only a fraction of those protein molecules exhibit a useful or active orientation, rendering most of the microarray useless in some cases. Thus, there has been a growing need for new chemistries offering greater selectivity within biological molecules to improve the utility of protein microarrays.

A major advance for protein chemistry occurred in 2001, when the Sharpless and Meldal Groups independently reported the selective copper-catalyzed reaction of azide and alkyne groups,[12,13] which was soon shown to be bioorthogonal (i.e., neither reactive partner interacts with chemical groups normally present in biological settings).[14] Numerous other bioorthogonal reactions have been established that enable selective and controlled chemical reactions of biomolecules.[15] Importantly, methods have been developed in concert to incorporate the appropriate chemical groups into proteins and other biomolecules, enabling their participation in bioorthogonal reactions.[16–20] One notable outcome of these interdisciplinary advances is that bioorthogonal reactions have now been utilized to achieve site-specific and selective immobilization of proteins on surfaces, as described in a recent review.[10] Clearly, much progress has been made since the Schreiber Lab's report of aldehyde–protein microarrays thirteen years ago.

Our objective for the work described here was to utilize NMT-mediated protein labeling as a step towards site-specific immobilization of functionalized proteins on surfaces for downstream applications. We developed methods using yARF-GFP, a protein from our original model system, and applied them to the CaN and hCaNB-CaM proteins described in Chapter III. Given that some surface immobilization techniques currently in use require purification of the protein of interest,[10] we were also intrigued by the possibility of coupling our recombinant proteins to surfaces directly from lysate. In general, the process of isolating a protein from lysate has three primary drawbacks: purification often requires considerable time and resources; it may result in a significant loss of net protein product; and it may cause adverse changes in protein structure and function. Thus, advancing methods for protein–surface coupling that do not require prior

protein purification is highly desirable. To that end, we describe our preliminary conjugation experiments with functionalized beads and a small-molecule dye, and then shift our focus to our work with protein microarrays.

RESULTS AND DISCUSSION

Experiments with Alkyne-Functionalized Agarose Beads

For all of our protein conjugation experiments, we planned to utilize the azide–alkyne cycloaddition reaction.[12,13,21] In order to gain a better understanding of how this reaction behaves when one partner is immobilized, we completed preliminary experiments with alkyne-functionalized agarose beads and a small-molecule azide dye. As shown in Figure IV-1, agarose beads displaying N-hydroxy succinimidyl (NHS) ester groups were reacted with amine-bearing alkyne reagents. Both acetylene (terminal alkyne) and azadibenzocyclooctyne (ADIBO) beads were prepared. Either ethanolamine or methyl-PEG4-amine was used to quench unreacted NHS groups; this quenching step is important for protein experiments, because NHS groups also react readily with lysine amine groups. Finally, beads were blocked with BSA or left unblocked. In total, eight types of alkyne-derivatized beads were prepared.

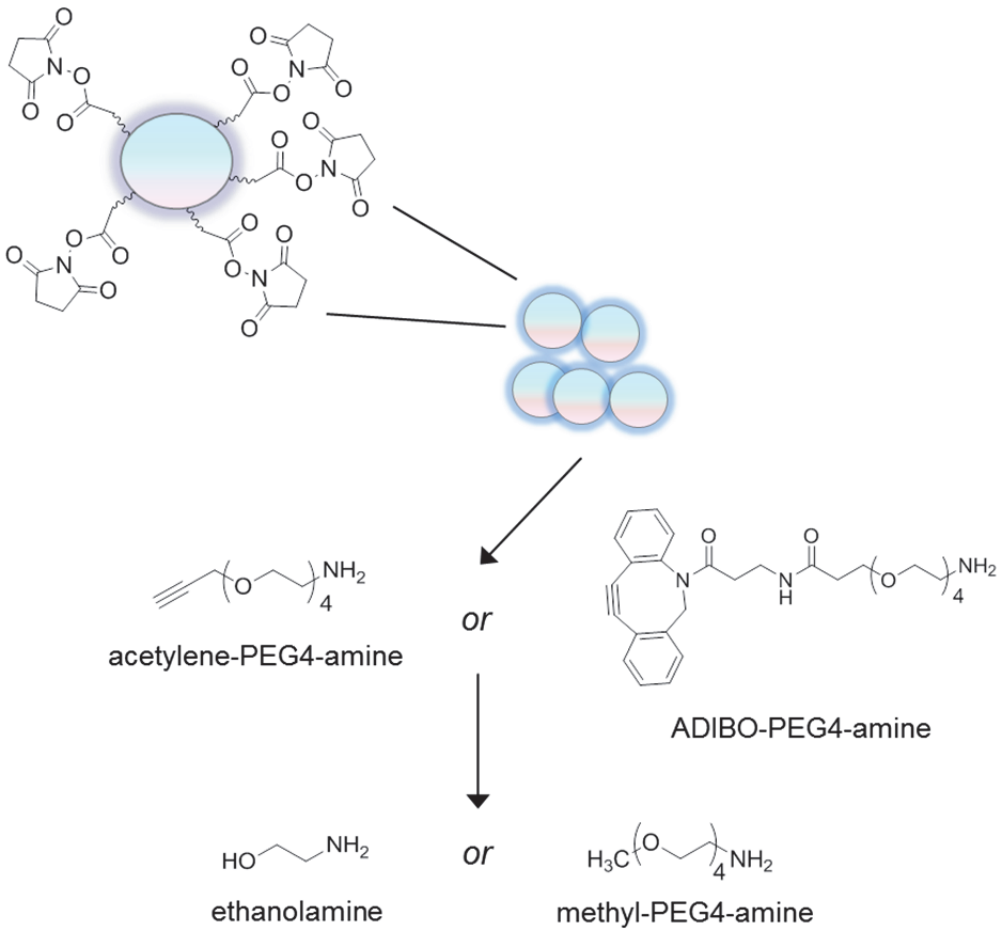

Figure IV-1. Schematic overview of functionalization of agarose beads. NHS-ester agarose beads were reacted with an acetylene or a cyclooctyne-bearing amine, followed by treatment with a quenching agent to ensure that no unreacted NHS-ester groups remained.

After completing the bead preparation protocol, we confirmed successful functionalization of the beads by reacting them with a small-molecule dye, Azide-Fluor488. We also wanted to determine whether or not the different quenching conditions and the BSA blocking step had any effect on azide-alkyne reaction efficiency. Either the copper-catalyzed or strain-promoted azide-alkyne reaction was carried out, depending on the bead type, with no-copper negative controls included for the acetylene

beads. Equivalent levels of fluorescence were observed across all four bead types for each type of alkyne (acetylene or ADIBO), indicating that functionalization was successful and that the type of quencher and the BSA blocking step did not affect reaction efficiency (data not shown). For subsequent experiments, we moved forward with both acetylene and ADIBO beads that had been quenched with methyl-PEG4-amine.

Next, we investigated how different bead preparation conditions affected the nonspecific binding of lysate protein to the beads. We hypothesized that the BSA blocking step would decrease nonspecific interaction of lysate proteins with the beads. We also expected to observe a higher background signal for ADIBO beads than for acetylene beads because the thiol groups in cysteine side chains are known to react with activated cyclooctynes.[22,23] To test these hypotheses, we reacted NHS-AlexaFluor633 with lysate protein collected from *E. coli* BL21(DE3) cells in which no protein expression had been induced, and we incubated beads with the dyed lysate. The fluorescence of the beads was measured before and after washing. The results, presented in Figure IV-2, indicate that the BSA blocking step did not have an impact on the interaction of our beads with lysate protein. However, ADIBO beads did indeed show a four-fold higher lysate background signal, even after washing, as compared to acetylene beads: it is likely that some lysate proteins react covalently with the ADIBO beads.

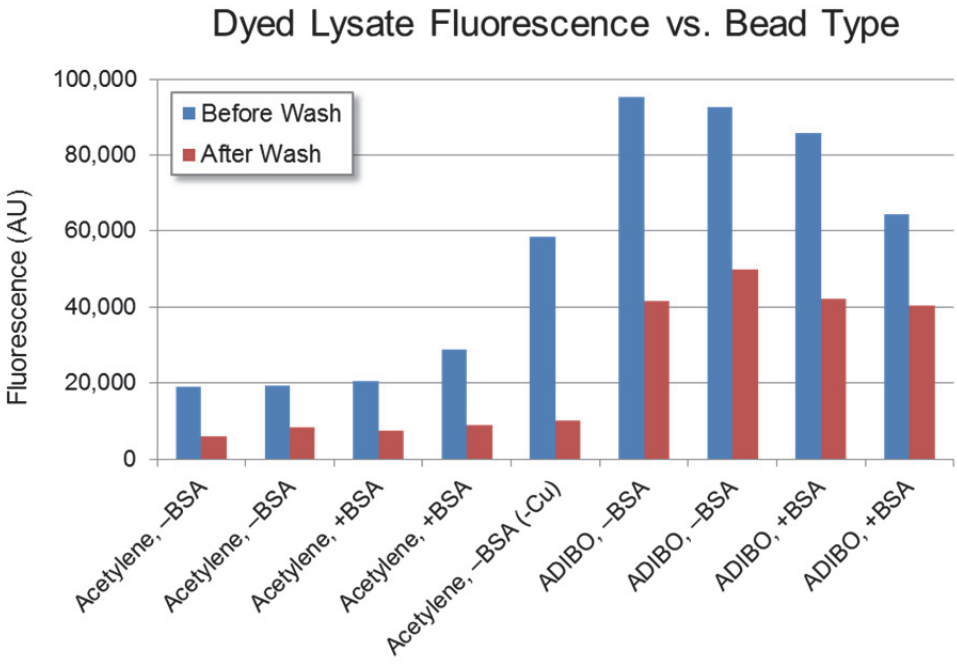

Figure IV-2. Fluorescence of beads after incubation with AlexaFluor633-dyed lysate, before/after washing. Duplicate pairs are shown for each bead type, except the no-Cu negative control. Beads were functionalized with acetylene-PEG4-amine or ADIBO-PEG4-amine, quenched with methoxy-PEG-amine, and blocked with BSA ("+BSA") or not blocked ("–BSA"). All fluorescence measurements were normalized by number of beads. After washing, roughly four times as much lysate remained on ADIBO beads as compared to acetylene beads.

We were also interested in how the presence of lysate protein affected the reaction efficiency between the azido dye and the alkynyl beads, an important consideration for achieving successful capture of 12-ADA-labeled proteins from lysate on alkyne-derivatized surfaces. Acetylene and ADIBO beads were reacted with Azide-Fluor488 in the absence (Figure IV-3A) or presence (Figure IV-3B) of lysate protein. We measured a two-fold lower fluorescence signal for beads that had been reacted with the azido dye in

the presence of lysate, for both acetylene and ADIBO beads. Again, very consistent results were obtained within each bead type, regardless of whether or not the beads had been blocked with BSA. These results were considered in the design of subsequent microarray experiments.

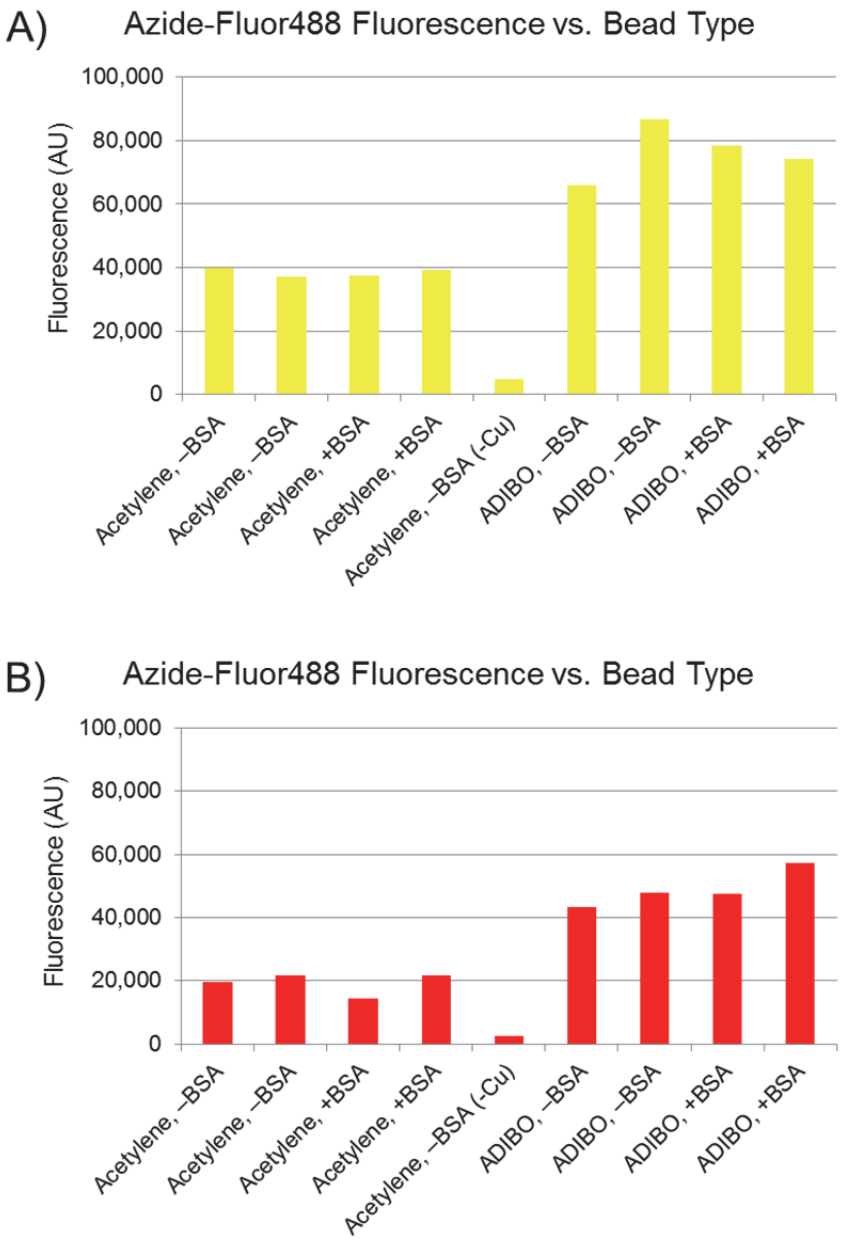

Figure IV-3. Fluorescence of beads after reaction with Azide-Fluor488 in the absence (A) or presence (B) of lysate. Duplicate pairs are shown for each bead type, except the no-Cu negative controls. Beads were functionalized with acetylene-PEG4-amine or ADIBO-PEG4-amine, quenched with methoxy-PEG-amine, blocked with BSA ("+BSA") or not blocked ("–BSA"), and washed, prior to reaction with Azide-Fluor488. All fluorescence measurements were normalized by number of beads. The azide-alkyne reaction yield in lysate is approximately half the reaction yield in buffer only.

Examination of the graphs in Figure IV-3 reveals a clear difference in average signal for ADIBO beads versus acetylene beads after reaction with Azide-Fluor488. Strained alkynes such as ADIBO are known to react with azides more rapidly and to a greater extent than terminal alkynes do.[24] However, as noted earlier and as evidenced by Figure IV-2, strained alkynes can also react nonspecifically with nucleophiles present in biological systems, particularly the thiol groups of Cys residues.[23] Thus, there is a trade-off between signal and background that is worth considering when selecting or designing an alkynyl molecule for reaction with azides, depending on the context of a given cycloaddition reaction. For our purposes, we found that the copper catalyst required for reaction of terminal alkynes with azides strongly interfered with activation of CaN by CaM (data not shown); both proteins possess multiple metal-binding centers, as discussed in Chapter III, so it is likely that either or both proteins bound the Cu^{2+} and Cu^{1+} ions yielded by the copper catalyst. Thus, we utilized cyclooctyne compounds exclusively when working with CaM and CaN, as described in the next section.

Overview of LFIRE Instrumentation and Experimental Set-up

In progressing from the use of an azido dye to the use of azide-labeled proteins, we also moved to a higher-throughput format than beads: protein microarrays. More specifically, a robotic spotter was used to print cyclooctyne molecules on glass slides at a density of approximately 16 spots per square mm, with a distance of 300 μm between spots. Glass slides were treated with a proprietary optical coating enabling their use in the Label-Free Internal Reflection Ellipsometry instrument, or LFIRE, developed by Maven Biotechnologies (Figure IV-4A).[25] The protocols for preparing amine-coated

glass slides and printing NHS-cyclooctyne molecules on the slides are described in more detail in the Experimental Section of this chapter.

Our LFIRE microarray experiments began with affixing a well structure to the printed slide, mounting the slide on a glass prism, and inserting the prism into the instrument (Figure IV-4B). The slide was kept hydrated and remained mounted on the prism throughout the experiment. Buffer was added to the wells, followed by a BSA blocking solution. LFIRE measurements were collected during this time to establish a consistent baseline. After the slide was thoroughly washed, cell lysate was added to each well, with simultaneous initiation of further LFIRE measurements. An image of the entire slide was collected with a predetermined frequency, depending on the size of the total printed area; for our experiments, an image was collected approximately once every 90 seconds. Data analysis entailed stacking all of the images in a software program such as ImageJ, subtracting a background image, and detecting localized rises in signal corresponding to protein deposition on the slide surface. The LFIRE experimental protocol is depicted schematically in Figure IV-4B, and the following sections describe our microarray work with 12-ADA-labeled yARF-GFP, CaN, and hCaNB-CaM.

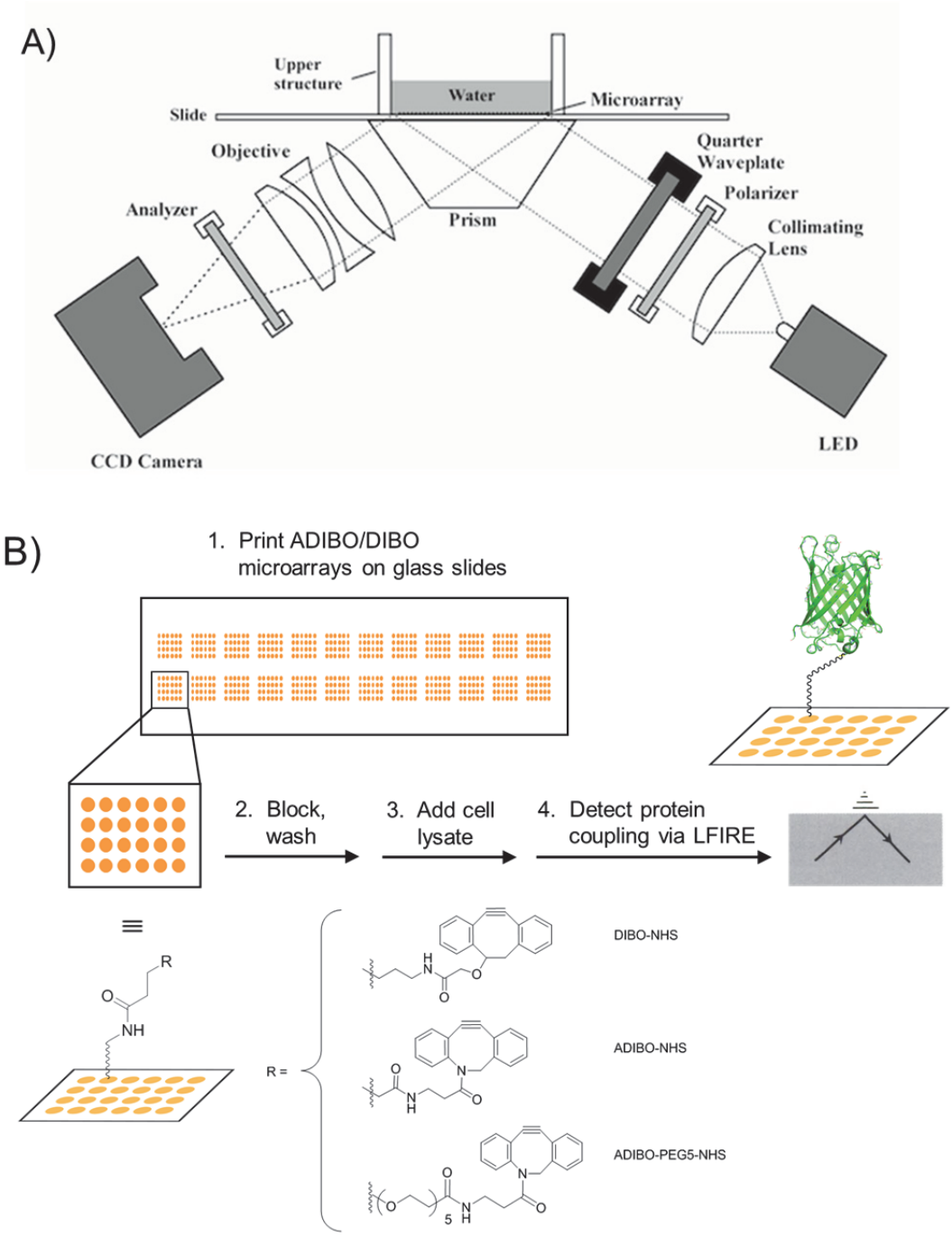

Figure IV-4. (A) Schematic overview of LFIRE instrument (adapted from Reference 25). Polarized light aids in the detection of changes in height, i.e., protein deposition, on the microarray surface. (B) Schematic overview of surface coupling experiments. Slides are printed with cyclooctyne spots, blocked, incubated with cell lysate, and imaged on the LFIRE.

Surface Capture and LFIRE Analysis of yARF-GFP Lysates

Lysates were prepared from *E. coli* cells in which yARF-GFP was expressed in the presence of no fatty acid, myristic acid, or 12-ADA; additionally, a negative control lysate was prepared from cells in which no test protein had been overexpressed. The protein concentration of each of the four lysate samples was measured, so that equal concentrations of lysate protein could be added to different wells on the microarray slide. For these experiments, we used slides that had been printed with DIBO-NHS or ADIBO-NHS (structures shown in Figure IV-4B). As described above, LFIRE data were collected throughout the duration of the blocking and lysate-coupling steps. Background-subtracted data are presented in Figures IV-5 and IV-6.

Analysis of the LFIRE data clearly indicated that significant coupling occurred only in the areas where DIBO or ADIBO was spotted, and only in wells to which lysate containing 12-ADA-yARF-GFP was added; the images shown in Figure IV-5 are representative of results obtained across multiple wells. Furthermore, the similarity in appearance of the control wells (no test protein, yARF-GFP, and Myr-yARF-GFP) indicates that the majority of background protein deposition is unlikely to be yARF-GFP, but rather, is likely the result of nonspecific reaction between cysteine-containing lysate proteins and DIBO or ADIBO. Finally, the large difference in appearance between Myr-yARF-GFP wells and 12-ADA-yARF-GFP wells demonstrates that the strong signal measured for the latter is not simply due to hydrophobic attraction between the fatty acid tag and the slide. Post-wash LFIRE data from multiple wells exposed to the same four lysate samples were analyzed quantitatively; those results are presented in Figure IV-6 and confirm that selective coupling is achieved with 12-ADA-yARF-GFP out of lysate.

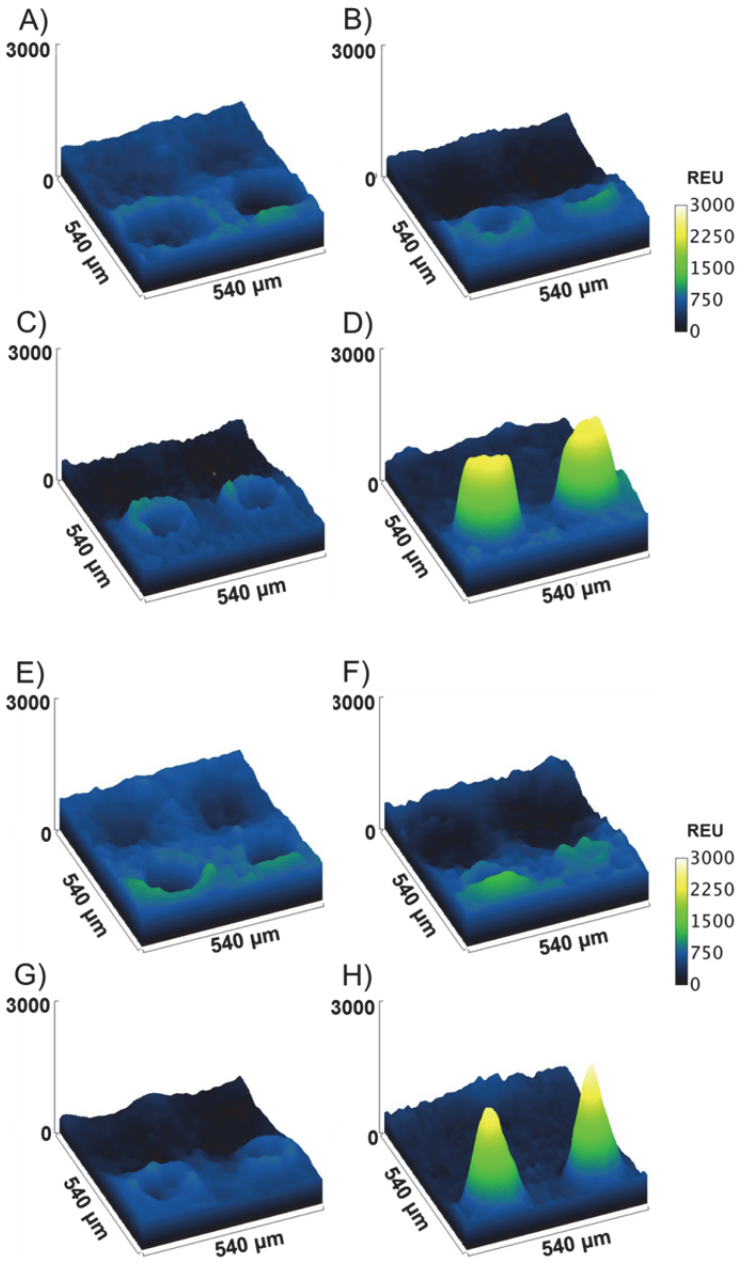

Figure IV-5. LFIRE 3-D surface plots of microarrays after incubation with cell lysate containing no overexpressed protein (A, E); yARF-GFP (B, F); Myr-yARF-GFP (C, G); or 12-ADA-yARF-GFP (D, H). The two microarray spots in back are BSA for all panels, and the two spots in front are DIBO (A–D) or ADIBO (E–H). Significant protein coupling was observed only in the presence of 12-ADA-labeled yARF-GFP lysate, and only within cyclooctyne-derivatized areas.

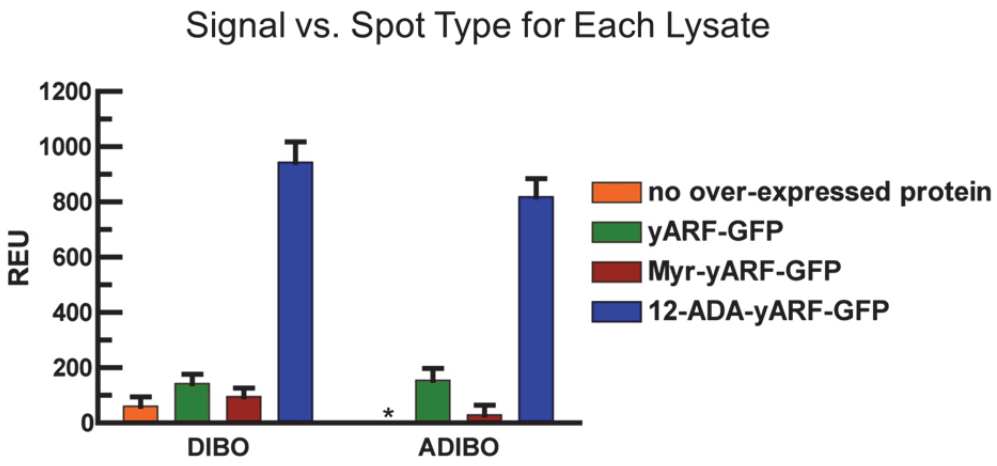

Figure IV-6. Average post-wash LFIRE signal for DIBO and ADIBO microarray spots after exposure to different lysate samples. For both DIBO and ADIBO slides, significant coupling was observed only in the presence of 12-ADA-labeled yARF-GFP. Each bar represents the average of $\geq$ 16 spots, $\pm$ standard error of the mean. * = no detectable signal.

Surface Capture and LFIRE Analysis of CaN Lysates

LFIRE experiments were performed with lysates containing Myr-CaN or 12-ADA-CaN in a manner similar to that described above for the yARF-GFP lysates. (Controls with no protein or unlabeled protein were not performed; attempts to express CaN in a non-myristoylated/non-labeled form have been shown to result in significant protein aggregation.[26]) Again, results indicated strong coupling only between cyclooctyne spots and 12-ADA-labeled protein (Figure IV-7). For these experiments, data analysis was performed before and after a final wash step. The strong post-wash signal observed in Figure IV-7B for 12-ADA-CaN, and its similarity to the pre-wash signal in Figure IV-7A, suggests that 12-ADA-CaN is covalently conjugated to the slide.

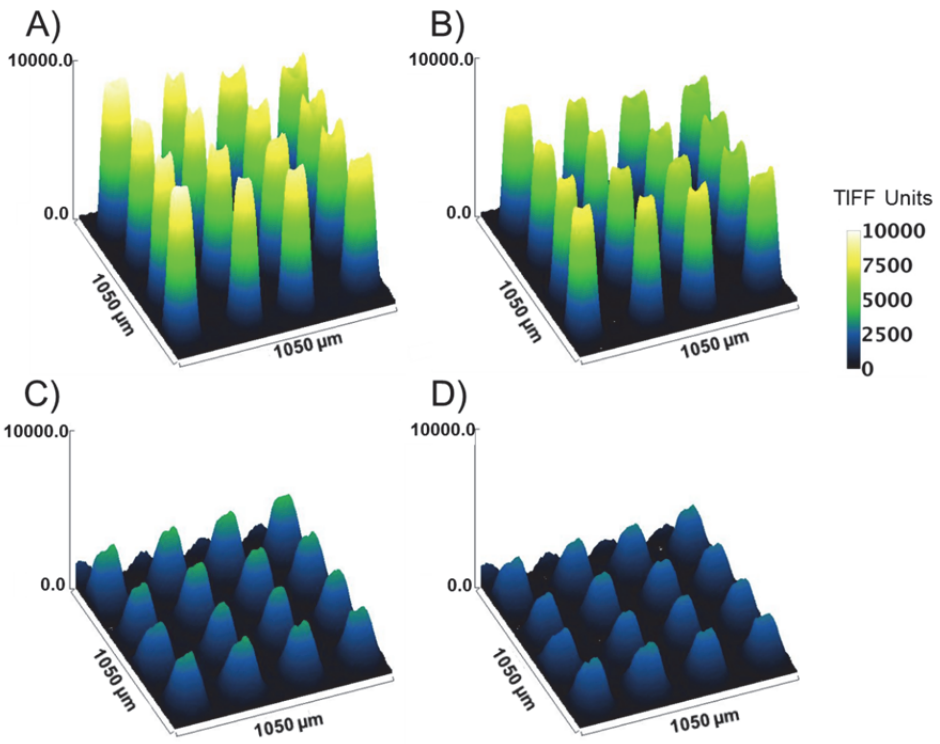

Figure IV-7. LFIRE 3-D surface plots of ADIBO-PEG5-NHS microarrays after incubation with cell lysate containing 12-ADA-CaN (A, B) or Myr-CaN (C, D). For all panels, the 16 spots shown are a representative subset from a larger array of 289 spots. (A) and (C) display signal immediately after incubation, prior to washing, while (B) and (D) display post-wash signal intensity. Significant protein coupling was observed only in the presence of 12-ADA-CaN, only within cyclooctyne-derivatized areas.

Further analysis of the CaN LFIRE data set was performed, as presented in Figure IV-8. Plotting the signal as a function of time provided insight into the relative efficiency of the azide-cyclooctyne reaction versus background reactions between cyclooctynes and other molecules present in lysate (Figure IV-8A). In particular, the data for the first 15 minutes of the incubation period indicate that the azide-cyclooctyne reaction proceeds considerably faster than background reactions in our system. Considering the significant

interest in and widespread use of the biocompatible azide-cyclooctyne reaction,[15,27] we believe these results could be of interest to the larger chemistry/chemical biology community.

We were also interested in gaining a better understanding of the enrichment factor achieved via protein coupling—that is, the amount of 12-ADA-labeled protein present on the slide versus present in lysate. As shown in Figure IV-8, the final signal of 12-ADA-CaN is roughly three times that of Myr-CaN: this result indicates that two-thirds of the 12-ADA-CaN signal corresponds to the labeled species, while one-third is background. Quantitative Western blotting indicated that CaN constitutes roughly 7% of the total lysate protein for both Myr-CaN and 12-ADA CaN (data not shown). Comparison of the ~7% figure in lysate (i.e., background:labeled = 93:7 = 13.3:1) with the ~66% figure after coupling (i.e., background:labeled = 34:66 = 0.51:1) yields a 26-fold reduction in contaminating proteins relative to 12-ADA-CaN upon coupling to cyclooctyne microarrays from lysate.

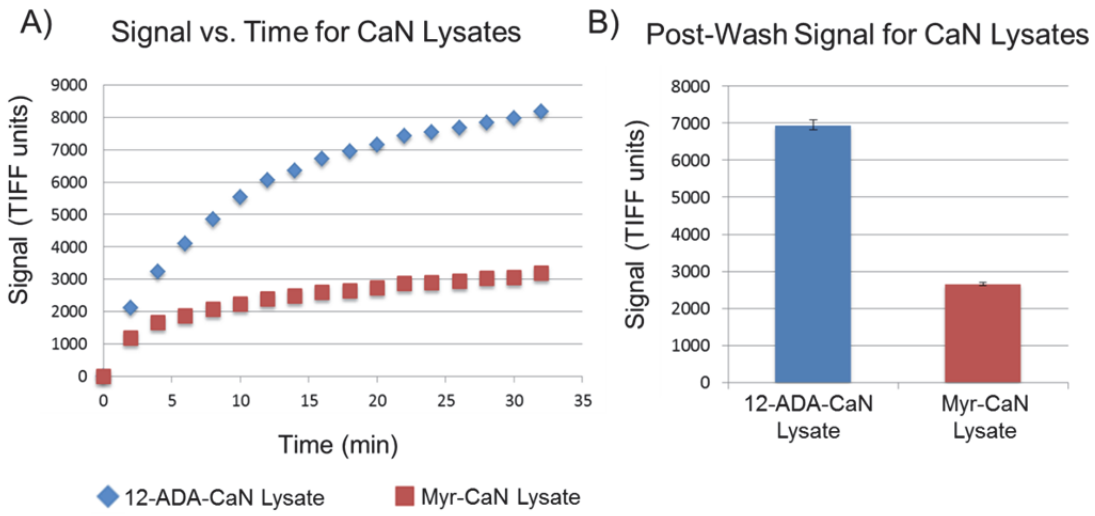

Figure IV-8. Quantitative analysis of CaN LFIRE surface plots. (A) Average signal for ADIBO microarray spots during incubation with lysate containing 12-ADA-CaN or Myr-CaN, prior to washing. Lysate was added at 0 min. (B) Average signal for ADIBO spots after lysate incubation and wash. For both panels, data points represent the average signal of the 16 spots shown in Figure IV-7. The results show that 12-ADA-CaN couples more quickly and more specifically to ADIBO spots as compared to the control protein, Myr-CaN. Error bars represent the standard deviation.

Surface Capture and LFIRE Analysis of hCaNB-CaM Lysates

Finally, LFIRE experiments similar to those outlined above were performed with lysates containing hCaNB-CaM expressed in the presence of myristic acid or 12-ADA; similar results were obtained as well. Lysate containing 12-ADA-labeled hCaNB-CaM (henceforth referred to as "12-ADA-CaM") coupled specifically to cyclooctyne spots, and the signal remained strong after washing (Figure IV-9, A and B). Lower signal intensities were detected for the negative control lysate containing myristoylated hCaNB-CaM (Myr-CaM) (Figure IV-9, C and D).

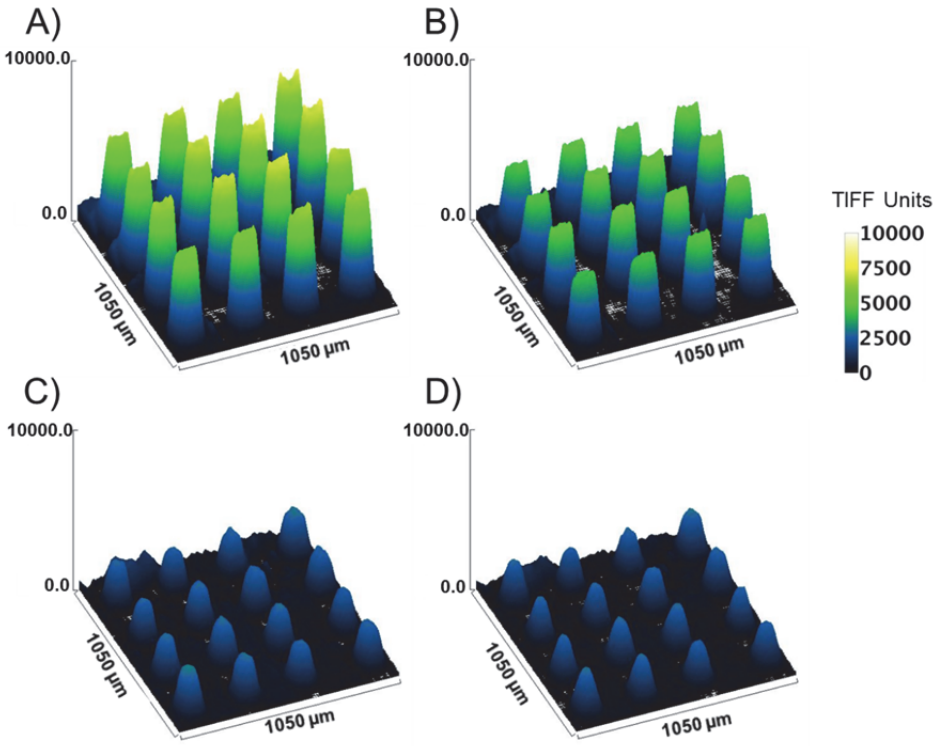

Figure IV-9. LFIRE 3-D surface plots of ADIBO-PEG5-NHS microarrays after incubation with cell lysate containing 12-ADA-CaM (A, B) or Myr-CaM (C, D). For all panels, the 16 spots shown are a representative subset from a larger array of 289 spots. (A) and (C) display signal immediately after incubation, prior to washing, while (B) and (D) display post-wash signal intensity. Significant protein coupling was observed only in the presence of 12-ADA-CaM, only within cyclooctyne-derivatized areas.

The representative images in Figure IV-9 indicate that the "signal-to-noise" ratio (final signal of 12-ADA-CaM versus final signal of Myr-CaM) is lower than the corresponding ratio for CaN, although the mass spectrometry results presented in Chapter III confirmed that both CaN and hCaNB-CaM are labeled quantitatively with 12-ADA. It is possible that the functionalized N-terminus of 12-ADA-CaM is less accessible for subsequent conjugation than that of 12-ADA-CaN; because CaN is a natural substrate of

NMT, it is likely that its native folded structure renders its N-terminus available for reaction. Further surface coupling studies with natural NMT substrate proteins and engineered substrates will elucidate the extent to which this theory is correct.

LFIRE data for the CaM lysates were also analyzed in a more quantitative manner (Figure IV-10). Again, we observed a more rapid reaction rate for the azide-cyclooctyne reaction than for background reactions, with the difference in reaction rates most apparent during the first 15 minutes (Figure IV-10A). As would be expected from the representative images shown in Figure IV-9, the average final post-wash signal of 12-ADA-CaM lysate is lower than that of 12-ADA-CaN lysate, though it is considerably higher than that of Myr-CaM lysate (Figure IV-10B). About 60% of the final signal for 12-ADA-CaM is the recombinant protein (i.e., background:labeled = 40:60 = 0.67:1). Quantitative Western blots of 12-ADA-CaM and Myr-CaM indicated that CaM constitutes ~13% of the total lysate protein (background:labeled = 87:13 = 6.7:1). Thus, we achieved a 10-fold reduction in contaminating proteins relative to 12-ADA-CaM upon coupling to cyclooctyne microarrays from lysate.

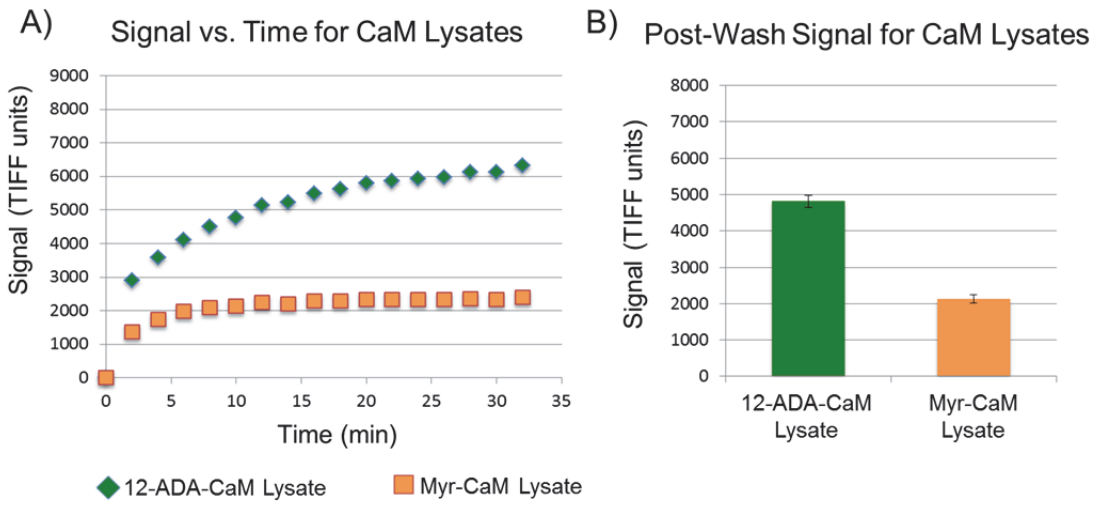

Figure IV-10. Quantitative analysis of CaM LFIRE surface plots. (A) Average signal for ADIBO microarray spots during incubation with lysate containing 12-ADA-CaM or Myr-CaM, prior to washing. Lysate was added at 0 min. (B) Average signal for ADIBO spots after lysate incubation and wash. For both panels, data points represent the average signal of the 16 spots shown in Figure IV-9. The results show that 12-ADA-CaM couples more quickly and more specifically to ADIBO spots as compared to the control protein, Myr-CaM. Error bars represent the standard deviation.

CONCLUSION

This chapter describes experiments completed with functionalized beads and microarrays, two different systems for surface capture of proteins. Using Maven Biotechnologies' LFIRE instrument, we detected selective coupling of 12-ADA-yARF-GFP, 12-ADA-CaN, and 12-ADA-hCaNB-CaM to cyclooctyne-spotted glass slides. The orthogonality exhibited by NMT toward bacterial proteins allowed us to couple 12-ADA-labeled proteins to derivatized surfaces directly out of lysate, a useful feature for studies

of proteins that are difficult to purify or that are negatively affected by isolation from the lysate environment. Experiments conducted with lysates containing no recombinant protein, unlabeled yARF-GFP, Myr-yARF-GFP, and 12-ADA-yARF-GFP resulted in significant surface coupling of 12-ADA-yARF-GFP only. The similar appearance of all three controls indicated that the coupling observed for 12-ADA-yARF-GFP was indeed specific to the azide moiety and was related to neither the protein sequence nor the presence of a fatty acid tag. Experiments conducted with 12-ADA-CaN and 12-ADA-CaM demonstrated that enrichment factors of 26 and 10, respectively, were achieved upon selective coupling of each protein from lysate to cyclooctyne arrays. These results provide a strong foundation for the completion of biochemical studies with CaN and CaM microarrays, as well as a set of methods for the surface capture of other proteins.

EXPERIMENTAL SECTION

Materials

Experiments with alkyne-derivatized agarose beads. NHS-ester agarose resin was purchased from GE Healthcare. Azide-Fluor488, Acetylene-PEG4-amine, and ADIBO-PEG4-amine were purchased from Click Chemistry Tools. Methyl-PEG4-amine was purchased from Pierce. Ethanolamine and fluorescein salt were purchased from Sigma-Aldrich. "Wash Buffer 1" was 1 mM HCl; "Wash Buffer 2" was 100 mM Tris-HCl, pH 8.5; "Wash Buffer 3" was 100 mM NaOAc, pH 4.5. "Coupling Buffer" was 200 mM $NaHCO_3$, 500 mM NaCl, pH 8.2. For CuAAC reactions, $CuSO_4$ was purchased from VWR, sodium ascorbate and aminoguanidine-HCl were purchased from Aldrich, and the ligand was bathophenanthroline sulfonated sodium salt from GFS Chemicals. For dye-labeling of lysate, NHS-AF633 (AlexaFluor-633 carboxylic acid, succinimidyl

ester) was purchased from Invitrogen. The BCA Assay kit was purchased from Pierce. Methanol, chloroform, and other solvents were purchased from VWR.

Cell lysate preparation. Bacterial cultures were grown as described in Chapters II and III. Lysis Buffer was composed of 50 mM Tris (pH 7.5), 100 mM NaCl, 0.1 mM PMSF, and Roche Complete Protease Inhibitor. OmniLyse cell lysis kits were purchased from Claremont BioSolutions. The BCA Assay kit was purchased from Pierce.

Amine functionalization of glass slides. Ammonium hydroxide was purchased from VWR. All other reagents were reagent grade and purchased from Sigma-Aldrich.

Microarray printing. "PBS-T" was composed of 50 mM phosphate, 150 mM NaCl, and 0.01% Tween-20. "TBS-T" was composed of 50 mM Tris (pH 7.5), 150 mM NaCl, and 0.01% Tween-20. The DIBO-NHS (Click-iT Succinimidyl Ester DIBO Alkyne) reagent was purchased from Life Technologies/Invitrogen. ADIBO-NHS and ADIBO-PEG5-NHS were purchased from Click Chemistry Tools. Methyl-PEG4-NHS (MS(PEG)4 succinimidyl ester) was purchased from Pierce. Anhydrous DMSO was purchased from Cambridge Isotope Laboratories. The SpotBot Personal Microarray System is manufactured by ArrayIt.

Methods

Experiments with alkyne-derivatized agarose beads. Beads were resuspended in the bottle, and 5 mL of slurry was transferred to a new conical vial. Packing buffer was removed, and beads were then washed 3 x 10 mL with Wash Buffer 1 and divided into two batches. Each batch was reacted with 25 mM acetylene-PEG4-amine or ADIBO-PEG4-amine in Coupling Buffer for 5 hr at room temperature. Quenching was accomplished with 100 mM ethanolamine or methyl-PEG4-amine in Coupling Buffer overnight at 4°C. Beads were then washed 3 x 10 mL alternating between Wash Buffers 2 and 3. Some beads were blocked with BSA (0.1% in 500 mM NaCl, pH 8.2). After a final set of washes with 500 mM NaCl, pH 8.2, beads were ready for reaction with the Azide-Fluor488 fluorescent probe.

To all beads, Azide-Fluor488 was added at a final concentration of 50 μM. For ADIBO-functionalized beads, no additional reagents were required. For acetylene-functionalized beads, CuAAC click reactions were performed as follows: 200 μM $CuSO_4$, 500 μM ligand, 5 mM sodium ascorbate, and 5 mM aminoguanidine-HCl (the Azide-Fluor488, $CuSO_4$, and ligand were combined separately and pre-mixed for 3 min). All reactions were performed in standard Phosphate-Buffered Saline (PBS). Reactions were allowed to proceed for 1.5 hr at room temperature, then beads were washed 8 times with PBS.

For experiments with dye-labeled lysate, *E. coli* BL21(DE3) cells were grown but no protein expression was induced. Cells were lysed in lysis buffer (1% SDS, 50 mM Tris-HCl, pH 8.0) according to the following formula: 50 μL lysis buffer per mL culture per OD_{600} unit. Lysate was dye-labeled with NHS-AF633 in PBS, then precipitated according to the methanol-chloroform precipitation protocol described in the Invitrogen Click-iT kit handbook. The protein pellets were resuspended in 8 M urea buffer, and protein concentration was measured using the BCA Assay kit. Dyed lysate was used at a concentration of 0.25 mg/mL in experiments with beads.

To measure the beads per unit volume, OD_{400} was measured on the plate reader. To measure the signal of Fluor488, samples were excited at 488 nm (bandwidth: 20 nm) and signal was read at 530 nm (bandwidth: 20 nm). To measure the signal of AF633, samples were excited at 633 nm (bandwidth: 5 nm) and signal was read at 660 nm (bandwidth: 5 nm). Fluorescence values were divided by OD_{400} values for normalization.

Cell lysate preparation. A cell pellet corresponding to approximately 5 mL of a given *E. coli* culture was resuspended in 500 μL Lysis Buffer at 4°C, lysed with mechanical disruption using OmniLyse cell lysis kits, and clarified of cellular debris via centrifugation (10 min x 10,000 *g* at 4°C). The concentration of soluble protein was determined with the BCA Assay kit. If lysates were not used the same day they were prepared, they were stored at -80°C and used within two weeks.

Amine functionalization of Maven glass slides. Microscope slides from Maven Biotechnologies were prepared for vapor phase deposition of APTES

((3-aminopropyl)triethoxysilane) by cleaning with RCA-1 (30% hydrogen peroxide, ammonium hydroxide, and RO water at a 1:1:10 ratio) and washing with DI water 3 times. Excess water was removed with N_2 gas, and slides were dried in an oven at 70-80°C for 1 hr. Slides were allowed to equilibrate to room temperature and placed in a vacuum desiccator. Then 2 microcentrifuge tubes, each containing 100 µL APTES, were placed inside the vacuum desiccator. The chamber was evacuated to 22 mm Hg and slides were incubated for at least 2 hr. Slides were stored at room temperature away from light prior to use.

Microarray printing. Microarrays were contact printed with a SpotBot Personal Microarray System using a 946 MP4 pin with approximately a 135 µm spot size on a 300 µm pitch. Microscope slides were washed 3 times with PBS-T and DI water and dried completely with N_2 gas. Control spots of 0.1 mg/mL BSA in TBS-T and 0.5 mg/mL polyethylene glycol (PEG, MW 35000) were printed, as were DIBO-NHS, ADIBO-NHS, ADIBO-PEG5-NHS, and methyl-PEG4-NHS in anhydrous DMSO and 0.5 mg/mL PEG. All arrays were printed in 55–65% humidity in under 1.5 hr. Spots were allowed to dry slowly in a humidified chamber, and slides were stored under N_2 gas with desiccant at -20°C.

LFIRE experiments with lysate samples. Maven amine-coated glass slides with printed microarrays were washed 3 times with PBS-T, mounted on a glass prism with index matching oil, and loaded into the LFIRE instrument. The optimal angle for the total internal reflection measurement, one that maximized the difference in signal between background and microarray spots, was determined. Each microarray was blocked with 0.25 mg/mL BSA in TBS-T for 1 hr and washed 5 times with TBS-T. Cell lysates containing recombinant proteins of interest were added at a final concentration of 0.5 mg/mL. The microarrays were incubated with lysates for approximately 1 hr, then washed 8 times with TBS-T. LFIRE data from each microarray were captured at approximately 80–120 second intervals throughout the experiment. All experiments were performed at room temperature.

LFIRE data analysis. The LFIRE instrument captures data in 16-bit grayscale TIFF units. These data were analyzed using the ImageJ software package. First, images from one experiment were placed in sequential order, stacked, and image stabilized. The image immediately preceding the addition of cell lysate was subtracted as a baseline from the sequence. Plots of the change in microarray surface and surface profile pixel intensities were generated using the Surface Plot and Plot Profile functions in ImageJ. To extract data from each microarray spot, regions of interest (ROIs) of uniform size were drawn around each spot, and the average pixel intensity from each ROI at each time point was exported to Microsoft Excel. For GFP-containing samples, data from replicate microarray spots were averaged and normalized to the average pixel intensity of the BSA spots, yielding data in relative ellipsometry units (REU). For CaN- and CaM-containing samples, data were not normalized to BSA spot intensities and are reported as TIFF units. All graphs were prepared with Prism software (GraphPad Software).

REFERENCES

1. Zhu, H. & Snyder, M. Protein arrays and microarrays. *Curr. Opin. Chem. Biol.* **5**, 40–5 (2001).

2. Espina, V. *et al.* Protein microarrays: molecular profiling technologies for clinical specimens. *Proteomics* **3**, 2091–100 (2003).

3. Zhu, H. & Qian, J. Chapter Four – Applications of Functional Protein Microarrays in Basic and Clinical Research. *Advances in Genetics* 123–55 (2012).

4. MacBeath, G. Protein microarrays and proteomics. *Nat. Genet. Supp.* **32**, 526–32 (2002).

5. Jason-Moller, L., Murphy, M. & Bruno, J. Overview of Biacore systems and their applications. *Curr. Protoc. Prot. Sci.* **19**, 1–14 (2006).

6. Ray, S., Mehta, G. & Srivastava, S. Label-free detection techniques for protein microarrays: prospects, merits and challenges. *Proteomics* **10**, 731–48 (2010).

7. Mehan, M. R. *et al.* Highly Multiplexed Proteomic Platform for Biomarker Discovery, Diagnostics, and Therapeutics. *Adv. Exp. Med. Biol.* **734**, 283–300 (2013).

8. Bertone, P. & Snyder, M. Advances in functional protein microarray technology. *FEBS J.* **272**, 5400–11 (2005).

9. Jenikova, G., Lao, U. L., Gao, D., Mulchandani, A. & Chen, W. Elastin-calmodulin scaffold for protein microarray fabrication. *Langmuir* **23**, 2277–9 (2007).

10. Chen, Y., Triola, G. & Waldmann, H. Bioorthogonal chemistry for site-specific labeling and surface immobilization of proteins. *Acc. Chem. Res.* **44**, 762–73 (2011).

11. MacBeath, G. & Schreiber, S. L. Printing proteins as microarrays for high-throughput function determination. *Science* **289**, 1760 (2000).

12. Rostovtsev, V. V, Green, L. G., Fokin, V. V & Sharpless, K. B. A stepwise huisgen cycloaddition process: copper(I)-catalyzed regioselective "ligation" of azides and terminal alkynes. *Angew. Chem. Int. Ed. Engl.* **41**, 2596–9 (2002).

13. Tornøe, C. W., Christensen, C. & Meldal, M. Peptidotriazoles on solid phase: [1,2,3]-triazoles by regiospecific copper(I)-catalyzed 1,3-dipolar cycloadditions of terminal alkynes to azides. *J. Org. Chem.* **67**, 3057–64 (2002).

14. Wang, Q. *et al.* Bioconjugation by copper(I)-catalyzed azide-alkyne [3 + 2] cycloaddition. *J. Am. Chem. Soc.* **125**, 3192–3 (2003).

15. Sletten, E. M. & Bertozzi, C. R. Bioorthogonal chemistry: fishing for selectivity in a sea of functionality. *Angew. Chem. Int. Ed. Engl.* **48**, 6974–98 (2009).

16. Duckworth, B. P., Zhang, Z., Hosokawa, A. & Distefano, M. D. Selective labeling of proteins by using protein farnesyltransferase. *ChemBioChem* **8**, 98–105 (2007).

17. Ngo, J. T. & Tirrell, D. A. Noncanonical amino acids in the interrogation of cellular protein synthesis. *Acc. Chem. Res.* **44**, 677–85 (2011).

18. Jing, C. & Cornish, V. Chemical tags for labeling proteins inside living cells. *Acc. Chem. Res.* **44**, 784–792 (2011).

19. Yao, J. Z. *et al.* Fluorophore targeting to cellular proteins via enzyme-mediated azide ligation and strain-promoted cycloaddition. *J. Am. Chem. Soc.* **134**, 3720–8 (2012).

20. Popp, M. W.-L., Karssemeijer, R. A. & Ploegh, H. L. Chemoenzymatic site-specific labeling of influenza glycoproteins as a tool to observe virus budding in real time. *PLoS Pathogens* **8**, e1002604 (2012).

21. Agard, N. J., Prescher, J. A. & Bertozzi, C. R. A strain-promoted [3 + 2] azide-alkyne cycloaddition for covalent modification of biomolecules in living systems. *J. Am. Chem. Soc.* **126**, 15046–7 (2004).

22. Beatty, K. E. *et al.* Live-cell imaging of cellular proteins by a strain-promoted azide-alkyne cycloaddition. *ChemBioChem* **11**, 2092–5 (2010).

23. Van Geel, R., Pruijn, G. J. M., Van Delft, F. L. & Boelens, W. C. Preventing thiol-yne addition improves the specificity of strain-promoted azide-alkyne cycloaddition. *Bioconjugate Chem.* **23**, 392–8 (2012).

24. Jewett, J. C. & Bertozzi, C. R. Cu-free click cycloaddition reactions in chemical biology. *Chem. Soc. Rev.* **39**, 1272–79 (2010).

25. LFIRE Technology. *Maven Biotechnologies* at <http://www.mavenbiotech.com/technology.htm>

26. Mondragon, A. *et al.* Overexpression and purification of human calcineurin alpha from Escherichia coli and assessment of catalytic functions of residues surrounding the binuclear metal center. *Biochemistry* **36**, 4934–42 (1997).

27. Sletten, E. M. & Bertozzi, C. R. From mechanism to mouse: a tale of two bioorthogonal reactions. *Acc. Chem. Res.* **44**, 666–76 (2011).